Diffusion Behavior of *n*-Alkanes by Molecular Dynamics Simulations

Geun Hoi Goo, Gihong Sung, Song Hi Lee,* and Taihyun Chang†

Department of Chemistry, Kyungsung University, Busan 608-736, Korea
†Department of Chemistry and Polymer Research Institute, Pohang University of Science and Technology, Pohang 790-784, Korea

Received April 16, 2002

In this paper we have presented the results of diffusion behavior of model systems for eight liquid *n*-alkanes (C_{12}-C_{44}) in a canonical (NVT) ensemble at several temperatures using molecular dynamics simulations. For these *n*-alkanes of small chain length *n*, the chains are clearly $\langle R_{ee}^2\rangle/6\langle R_g^2\rangle > 1$ and non-Gaussian. This result implies that the liquid *n*-alkanes over the whole temperatures considered are far away from the Rouse regime, though the ratio becomes close to the unity as *n* increases. Calculated self-diffusion constants D_{self} are comparable with experimental results and the Arrhenius plot of self-diffusion constants versus inverse temperature shows a different temperature dependence of diffusion on the chain length. The global rotational motion of *n*-alkanes is examined by characterizing the orientation relaxation of the end-to-end vector and it is found that the ratio τ_1/τ_2 is less than 3, the value expected for a isotropically diffusive rotational process. The friction constants ζ of the whole molecules of *n*-alkanes are calculated directly from the force auto-correlation (FAC) functions and compared with the monomeric friction constants ζ_D extracted from D_{self}. Both the friction constants give a correct qualitative trends: decrease with increasing temperature and increase with increasing chain length. The friction constant calculated from the FAC's decreases very slowly with increasing temperature, while the monomeric friction constant varies rapidly with temperature. By considering the orientation relaxation of local vectors and diffusion of each site, it is found that rotational and translational diffusions of the ends are faster than those of the center.

Key Words : Molecular dynamics simulation, Diffusion coefficient, *n*-Alkanes

Introduction

It is well known that dynamics of polymer chains such as self-diffusion constant, D_{self}, and zero shear viscosity, η_o, for a melt of chains shows three distinctively different behaviors according to the molecular weight or the chain length. The first crossover is from the behavior of unentangled chain regime to that of entangled polymer regime:[1]

$$D_{self} \sim M^{-1} \text{ and } \eta_o \sim M^1 \text{ for } M<M_c \qquad (1)$$
$$D_{self} \sim M^{-2} \text{ and } \eta_o \sim M^{3.4} \text{ for } M>M_c,$$

where M_c is the entanglement coupling molecular weight. The polymer chain dynamics of unentangled and entangled chains are commonly described by the Rouse and the reptation model, respectively.[2,3] The second crossover is from the behavior of very small *n*-alkane molecules to the Rouse regime. The study of *n*-alkanes in the range of medium size (C_{20}-C_{40}) provides a clue for the simplest physical system for investigating the Rouse regime of polymer dynamics. The first crossover has received considerable attention in recent years,[3,4] while the second crossover has received relatively little attention.

At the molecular weight below the Rouse regime, D_{self} and η_o of *n*-alkanes show power law behaviors. For example, D_{self} of *n*-alkanes from *n*-octane to polyethylene of the molecular weight of several thousands was reported to follow the relation, D_{self}~$M^{-\alpha}$ in which the exponents α is in the range of 2.72-1.75 depending on temperature.[5-7] Although the power law dependence has the same functional form as in Eq. (1), the origin is totally different. The molecular weight dependence of D_{self} and η_o in Eq. (1) is attributed to the topological entanglement effect not the segmental friction while the exponent α found below the Rouse regime reflects the molecular weight dependence of the local friction not the topological effect. A property often employed to investigate the local friction in the polymer chain dynamics is the monomeric friction coefficient, ζ_o. For low molecular weight polymers, ζ_o depends on the molecular weight. Above the onset molecular weight at which the Rouse behavior is observed, ζ_o becomes independent of molecular weight.[1,4] Recent molecular dynamics (MD) simulation studies showed that the Rouse chain behavior of *n*-alkane was obtained around 80 carbons at which ζ_o reaches an asymptotic limit independent of molecular weight.[8,9]

In a recent study,[10] diffusion of methyl yellow (MY) in the oligomeric host of *n*-alkanes and *n*-alcohols was studied by forced Rayleigh scattering as a function of the molecular weight and the viscosity of the medium. It was observed that the diffusivity of the probe molecule follows a power law dependence on the molecular weight of the oligomers, D_{MY}~$M^{-\alpha}$ well. As the molecular weight of the oligomers increases, the exponent shows a sharp transition from 1.88 to 0.91 near docosane (C_{22}) in *n*-alkanes and from 1.31 to 0.60 near 1-hexadecanol ($C_{16}OH$) in *n*-alcohols at 45 C. A similar transition was also found in the molecular dynamics (MD) simulation for the diffusion of a Lennard-Jones particle of a size similar to MY in *n*-alkanes. This transition deems to reflect a change of the dynamics of oligomeric chain molecules that the motion of the segments, not the entire molecules, becomes responsible for the transport of the probe molecule as the molecular weight of the oligomer increases.

In this study we have investigated the diffusion behavior of small *n*-alkane molecules by MD simulation in a canonical (NVT) ensemble at temperatures of 273, 293, 311, 333, and 372 K. We have chosen 8 liquid n-alkane systems of various chain lengths, $12 \le n \le 44$. The primary purpose of this work is to characterize the diffusion dynamics of small size *n*-alkanes as a function of chain length *n* (or molecular weight M) and as a function of temperature. In general the temperature dependence of the diffusion constant of small *n*-alkane is well described by the Arrhenius equation. The Arrhenius behavior of the small *n*-alkanes over the whole temperatures considered is examined and the diffusion activation energies of the Arrhenius plot for the given *n*-alkanes are determined. We also try to investigate the local intramolecular relaxation by considering the orientation relaxation of local vectors and local diffusion of monomers at both center and end monomers.

This paper is organized as follows: In Section II, we present the molecular models and NVT MD simulation methods. We discuss our simulation results in Section III and present the concluding remarks in Section IV.

Molecular Models and MD Simulation Methods

For *n*-alkanes, we have chosen 8 systems - *n*-dodecane ($C_{12}H_{26}$), *n*-hexadecane ($C_{16}H_{34}$), *n*-eicosane ($C_{20}H_{42}$), *n*-tetracosane ($C_{24}H_{50}$), *n*-octacosane ($C_{28}H_{58}$), *n*-dotriacontane ($C_{32}H_{66}$), *n*-hexatriacontane ($C_{36}H_{74}$), and *n*-tetratetracontane ($C_{44}H_{90}$). Each simulation was carried out in the NVT ensemble; the number of *n*-alkane was N=100, the density and hence the length of cubic simulation box were fixed and listed in Table 1 with given temperatures. The usual periodic boundary condition in the x-, y-, and z-directions and the minimum image convention for pair potential were applied. Gaussian isokinetics was used to keep the temperature of the system constant.[11,12]

We used a united atom (UA) model for *n*-alkanes, that is, methyl and methylene groups are considered as spherical interaction sites centered at each carbon atom. This model was used in the previous simulation studies.[13-17] Here, we briefly describe the salient features of the model. The interaction between the sites on different *n*-alkane molecules and between the sites separated by more than three bonds in the same *n*-alkane molecule was described by a Lennard-Jones (LJ) potential. All the sites in a chain have the same LJ size parameter $\sigma_i \equiv \sigma_{ii} = 3.93$ Å, and the well depth parameters were $\varepsilon_i \equiv \varepsilon_{ii} = 0.94784$ kJ/mol for interactions between the end sites and $\varepsilon_i = 0.39078$ kJ/mol for interactions between the internal sites. The Lorentz-Berthelot combining rules [$\varepsilon_{ij} \equiv (\varepsilon_i\varepsilon_j)^{1/2}$, $\sigma_{ij} \equiv (\sigma_i + \sigma_j)/2$] were used for interactions between an end site and an internal site. A cut-off distance of $2.5\sigma_i$ was used for all the LJ interactions.

Initially the bond-stretching was described by a harmonic potential, with an equilibrium bond distance of 1.54 Å and a force constant of 1882.8 kJ/mol/Å^2. The bond bending interaction was also described by a harmonic potential with an

Table 1. MD simulation parameters for molecular models of *n*-alkanes

n-alkanes	T (K)	Density (g/mL)^a	Length of box (Å)	*n*-alkanes	T (K)	Density (g/mL)^a	Length of box (Å)
n-$C_{12}H_{26}$	273	0.7636	33.335	*n*-$C_{16}H_{34}$	273	0.7874	36.281
(14.195)^b	293	0.7487	33.555	(14.153)^b	293	0.7737	36.494
(5.0 ns)^c	311	0.7360	33.747	(5.0 ns)^c	311	0.7612	36.692
	333	0.7194	34.004		333	0.7460	36.940
	372	0.6907	34.469		372	0.7190	37.396
n-$C_{20}H_{42}$	273	0.8021	38.819	*n*-$C_{24}H_{50}$	273	0.8118	41.070
(14.128)^b	293	0.7888	39.036	(14.111)^b	293	0.7988	41.292
(5.0 ns)^c	311	0.7769	39.234	(5.0 ns)^c	311	0.7873	41.492
	333	0.7621	39.486		333	0.7728	41.750
	372	0.7361	39.946		372	0.7475	42.215
n-$C_{28}H_{58}$	273	0.8196	43.086	*n*-$C_{32}H_{66}$	273	0.8243	44.951
(14.099)^b	293	0.8068	43.312	(14.090)^b	293	0.8119	45.179
(7.5 ns)^c	311	0.7918	43.584	(7.5 ns)^c	311	0.8007	45.388
	333	0.7776	43.847		333	0.7869	45.653
	372	0.7565	44.252		372	0.7626	46.132
n-$C_{36}H_{74}$	273	0.8296	46.644	*n*-$C_{44}H_{90}$	273	0.8296	49.697
(14.083)^b	293	0.8171	46.880	(14.073)^b	293	0.8249	49.953
(10.0 ns)^c	311	0.8059	47.096	(15.0 ns)^c	311	0.8135	50.185
	333	0.7921	47.369		333	0.7993	50.480
	372	0.7677	47.865		372	0.7745	51.014

^{a}Densities of *n*-alkanes are obtained from or interpolated (or extrapolated) from the values at liquid states in Ref. 33. ^{b}Mass of monomer (g/mole). ^{c}Equilibration time.

equilibrium angle of 114° and a force constant of 0.079187 kJ/mol/degree^2. The torsional interaction was described by the potential developed by Jorgensen *et al.*[18]:

$$U_{torsion}(\phi) = a_0 + a_1 \cos\phi + a_2 \cos^2\phi + a_3 \cos^3\phi \qquad (2)$$

where ϕ is the dihedral angle, and a_0 = 8.3973 kJ/mol, a_1 = 16.7862 kJ/mol, a_2 = 1.1339 kJ/mol, and a_3 = -26.3174 kJ/mol. For the time integration of the equations of motion, we adopted Gear's fifth-order predictor-corrector algorithm[19] with a time step of 0.5 femto-second for all the systems. Later the bond-stretching was switched to a constraint force which keeps intramolecular nearest neighbors at a fixed distance. The advantage for this change is to increase the time step as 5 femto-seconds with the use of RATTLE algorithm.[20] After a total of 1,000,000 time steps (5.0 nano-seconds) for equilibration, the equilibrium properties were then averaged over 5 blocks of 200,000 time steps (1.0 nano-seconds) but more equilibration time was required for longer chains greater than n = 24 and the required equilibration time for each chain was listed in Table 1. The configurations of all the molecules for further analyses were stored every 10 time steps (0.05 nano second) which is small enough for the tick of any time auto- correlation functions.

There are two routes to determine self-diffusion constants

Table 2. Static and dynamic properties of *n*-alkanes. Uncertainties in the last reported digit(s) are given in parenthesis

n-alkanes	T (K)	R_g^2 (Å^2)	R_{ee}^2 (Å^2)	$R_{ee}^2/6R_g^2$	*trans* %	D_{self}(MSD)^a	D_{self}(VAC)	ζ^b	$\zeta_{D(MSD)}$
n-$C_{12}H_{26}$	273	15.8(2)	140(3)	1.48	75.4(18)	7.61(45)	7.47(59)	180(0)	249(15)
(-0.60)^c	293	15.6(2)	136(3)	1.45	73.8(13)	10.6(6)	10.4(11)	179(0)	192(11)
	311	15.4(2)	134(3)	1.45	72.5(16)	14.1(4)	13.7(17)	177(0)	153(4)
	333	15.2(2)	131(3)	1.44	70.8(20)	19.3(6)	20.7(16)	176(1)	120(4)
	372	14.9(2)	127(3)	1.42	68.7(22)	27.5(6)	30.2(24)	175(1)	93.7(20)
n-$C_{16}H_{34}$	273	26.3(5)	235(6)	1.49	76.2(17)	3.86(15)	3.41(17)	243(0)	368(14)
(-0.83)^c	293	25.7(3)	227(7)	1.47	74.1(15)	6.02(37)	5.61(36)	241(0)	253(16)
	311	25.4(4)	223(6)	1.46	73.0(16)	8.25(49)	8.09(47)	239(0)	196(17)
	333	24.9(4)	215(7)	1.44	71.3(18)	11.6(2)	11.0(13)	238(0)	149(3)
	372	24.2(4)	206(7)	1.42	68.9(19)	18.3(3)	18.5(13)	236(1)	106(2)
n-$C_{20}H_{42}$	273	38.2(6)	342(16)	1.49	76.5(16)	2.31(18)	2.03(32)	305(0)	492(38)
(-1.01)^c	293	37.6(8)	330(13)	1.46	74.6(16)	3.70(23)	3.25(15)	303(0)	329(20)
	311	36.8(5)	318(10)	1.44	73.1(14)	5.54(16)	5.20(34)	301(0)	233(7)
	333	35.8(7)	306(12)	1.42	71.4(15)	7.74(26)	7.31(49)	299(1)	179(6)
	372	34.7(6)	292(11)	1.40	69.0(16)	13.0(6)	12.7(9)	297(2)	119(5)
n-$C_{24}H_{50}$	273	52.1(11)	466(17)	1.49	77.7(16)	1.60(15)	1.35(23)	367(1)	591(55)
(-1.17)^c	293	50.9(10)	453(17)	1.45	75.0(11)	2.55(18)	2.27(23)	365(0)	398(28)
	311	49.7(11)	427(16)	1.43	73.2(14)	3.75(16)	3.51(21)	362(1)	287(12)
	333	48.2(11)	405(17)	1.40	71.4(14)	5.40(26)	5.12(19)	360(0)	214(10)
	372	46.5(10)	386(16)	1.38	69.2(15)	9.79(33)	9.18(64)	357(1)	132(4)
n-$C_{28}H_{58}$	273	67.2(10)	597(19)	1.48	77.9(16)	1.13(7)	1.00(10)	430(1)	718(44)
(-1.37)^c	293	64.8(14)	559(21)	1.44	75.2(12)	1.91(10)	1.66(25)	427(1)	456(24)
	311	63.1(14)	529(20)	1.40	73.4(14)	2.92(20)	2.46(44)	424(0)	316(22)
	333	61.4(12)	509(24)	1.38	71.6(13)	4.33(10)	4.13(31)	421(1)	228(5)
	372	58.6(13)	476(20)	1.35	69.5(13)	7.38(39)	6.67(70)	417(1)	150(8)
n-$C_{32}H_{66}$	273	85.4(25)	752(24)	1.47	78.5(20)	0.93(6)	0.80(8)	490(1)	763(49)
(-1.95)^c	293	82.1(23)	709(19)	1.44	76.0(17)	1.41(5)	1.29(11)	488(1)	540(19)
	311	79.0(24)	649(25)	1.37	73.6(11)	2.07(6)	1.85(16)	486(1)	390(11)
	333	75.6(19)	610(27)	1.34	71.8(12)	3.17(26)	3.17(18)	482(1)	273(22)
	372	70.5(22)	558(26)	1.32	69.8(12)	6.15(26)	6.02(21)	478(1)	157(7)
n-$C_{36}H_{74}$	273	108(27)	929(28)	1.43	79.2(29)	0.76(5)	0.61(11)	555(2)	830(55)
(-2.35)^c	293	100(27)	844(30)	1.40	76.6(12)	1.16(5)	1.08(15)	551(1)	584(25)
	311	95.6(21)	774(31)	1.35	73.6(13)	1.68(11)	1.50(9)	547(1)	427(28)
	333	90.9(22)	728(31)	1.33	72.1(11)	2.68(13)	2.42(16)	544(1)	287(14)
	372	85.0(20)	666(25)	1.31	70.3(12)	5.12(33)	4.92(36)	538(1)	168(11)
n-$C_{44}H_{90}$	273	149(32)	1225(38)	1.37	81.2(16)	0.52(5)	0.36(7)	675(1)	993(95)
(-2.94)^c	293	136(30)	1107(32)	1.35	77.5(14)	0.84(6)	0.66(10)	673(1)	659(47)
	311	127(29)	1006(37)	1.32	74.7(11)	1.21(7)	1.01(7)	671(1)	486(28)
	333	121(24)	937(31)	1.29	76.1(11)	1.93(16)	1.64(29)	666(1)	326(27)
	372	111(29)	842(31)	1.26	70.9(12)	3.69(11)	3.40(23)	660(1)	191(6)

^{a}In 10^{-6} cm^2/sec. ^{b}In g/(ps·mol). ^{c}The expansion coefficient in 10^{-3} K^{-1}.

of n-alkanes from MD simulations: the Einstein relation from the mean square displacement (MSD).[21]

$$D_{self} = \frac{1}{6}\lim_{t\to\infty}\frac{d\langle|\mathbf{r}(t)-\mathbf{r}(0)|\rangle^2}{dt}. \tag{3}$$

and the Green-Kubo relation from the velocity autocorrelation (VAC) function of n-alkanes.[21]

$$D_{self} = \frac{1}{3}\int_0^\infty \langle \mathbf{v}_i(t)\cdot\mathbf{v}_i(0)\rangle dt. \tag{4}$$

Results and Discussion

Structural properties. Some equilibrium properties for liquid n-alkanes at 273, 293, 311, 333, and 372 K obtained from our MD simulations are listed in Tables 2 and 3. The calculated square radii of gyration (R_g^2) and the square end-to-end distances (R_{ee}^2) of n-tetracosane (C_{24}) at 333 and 372 K are in good agreement with the pervious MD simulation results[22] for a united atom (UA) model [48.9(0.3) and 409(6) at 333 K and 46.3(0.3) and 376(5) at 372 K, respectively]. The slight difference of both R_g^2 and R_{ee}^2 is probably due to the difference in the running times. In all cases decrease of both R_g^2 and R_{ee}^2 with increasing temperature was found.

The crossover of the square radii of gyration and the square end-to-end distances to the Rouse regime is examined as a function of the chain length, n. For Gaussian chains, it is satisfied that $<R_{ee}^2> = 6<R_g^2> = nb^2$ where b is the effective bond length. The ratios of $<R_{ee}^2>/6<R_g^2>$ for liquid n-alkanes at several temperatures obtained from our MD simulations are shown in Table 2. Clearly the ratio decreases with increasing temperature for all n-alkanes considered. At low temperatures for small $n < 16$, the ratio increases with increasing n since the chains are relatively rigid for small n. At 372 K, the ratio constantly decreases with increasing n and it also does at 333 K except C_{12}. In the case of n-alkanes studied here, the chains are clearly $<R_{ee}^2>/6<R_g^2>>1$ and non-Gaussian. For n-alkanes, the crossover to Gaussian chain statistics is known to occur for n greater than 100.[23-25] Since the Rouse model is based on the fact that the chains are Gaussian, one would expect that the crossover length is a minimum chain length for the Rouse model to hold, though this has not previously been checked systematically. Hence data from Table 2 for the ratio of $<R_{ee}^2>/6<R_g^2>$ implies that the liquid n-alkanes over the whole temperatures considered are far away from the Rouse regime.

The change of R_g^2 over the whole temperature interval can be used to obtain an estimate of the expansion coefficient $k = d(\ln R_g^2)/dT$, which is given in Table 2. We also plot ($\ln R_g^2$) versus temperature in Figure 1. The obtained expansion coefficient n-tetracosane (C_{24}) at 333 K is also in good agreement with the pervious MD simulation results[22] for the UA model ($k = -1.10.2 \times 10^{-3}$ K^{-1}). The corresponding experimental value for bulk polyethylene $k = -1.07 \pm 0.08 \times 10^{-3}$ K^{-1}, obtained SANS measurements.[26] In general we find a decrease of the expansion coefficient with increasing temperature. The average % of C-C-C-C *trans* is found to decrease with increasing temperature which is coincided with the decrease of both R_g^2 and R_{ee}^2, but it increases with increasing chain length. As temperature increases, there is a reduction in the degree of asymmetry for n-dodecane (C_{12}) and n-tetracosane (C_{24}), as shown by a decrease of the largest eigenvalues (l_1^2) of the mass tensor listed in Table 3. l_1 corresponds to the smallest eigenvalue of the inertia tensor and the associated eigenvector defines the direction of the longest principal axis of the molecule's ellipsoid of inertia.[27] These eigenvalues (l_i^2) satisfy the relation $l_1^2 + l_2^2 + l_3^2 = R_g^2$ with $l_1^2 > l_2^2 > l_3^2$. The largest eigenvalues (l_1^2) of the mass tensor also decreases with increasing chain length.

Diffusion constants. Self-diffusion constants, D_{self}, obtained from both the Einstein relation, Eq. (5), from the

Table 3. Some selected properties of n-alkanes. Uncertainties in the last reported digit are given in parenthesis

n-alkanes	T (K)	l_1^2/R_g^2	l_2^2/R_g^2	$\tau_1(ee)^a$	$\tau_2(ee)$	$\tau_1(c)$		$\tau_1(a)$		$\tau_1(b)$	
						ctr	end	ctr	end	ctr	end
n-$C_{12}H_{26}$	273	0.919(6)	0.069(5)	170	62.0	169	157	15.7	13.8	15.8	14.9
	293	0.915(6)	0.072(5)	109	38.9	111	105	11.7	10.4	11.3	10.1
	311	0.911(6)	0.075(6)	82.8	30.2	83.2	81.8	9.1	8.1	9.0	8.7
	333	0.906(6)	0.079(6)	56.2	21.4	55.3	54.2	7.5	7.0	7.7	7.3
	372	0.901(7)	0.084(6)	36.4	12.9	39.4	38.1	5.8	5.5	5.8	5.4
n-$C_{24}H_{50}$	273	0.892(8)	0.094(7)	1880	663	652	303	56.0	34.9	56.9	31.0
	293	0.885(7)	0.100(6)	1160	409	458	195	44.1	21.3	42.5	19.8
	311	0.876(9)	0.107(8)	735	269	381	159	32.3	18.9	33.6	19.4
	333	0.866(10)	0.116(9)	466	170	300	131	21.7	9.4	20.5	9.0
	372	0.860(9)	0.120(8)	244	92.4	211	95.6	12.9	7.2	11.9	6.4
n-$C_{44}H_{90}$	273	0.855(7)	0.127(6)	6660	2560	1020	403	95.6	48.5	93.3	47.2
	293	0.850(8)	0.128(6)	3570	1360	646	290	61.9	36.4	62.6	37.3
	311	0.846(9)	0.129(8)	2540	978	535	222	45.2	19.8	45.0	19.7
	333	0.838(3)	0.132(3)	1500	577	465	168	30.4	10.4	29.7	9.9
	372	0.828(3)	0.139(3)	812	320	308	126	16.7	5.7	17.3	5.7

^{a}In the unit of ps.

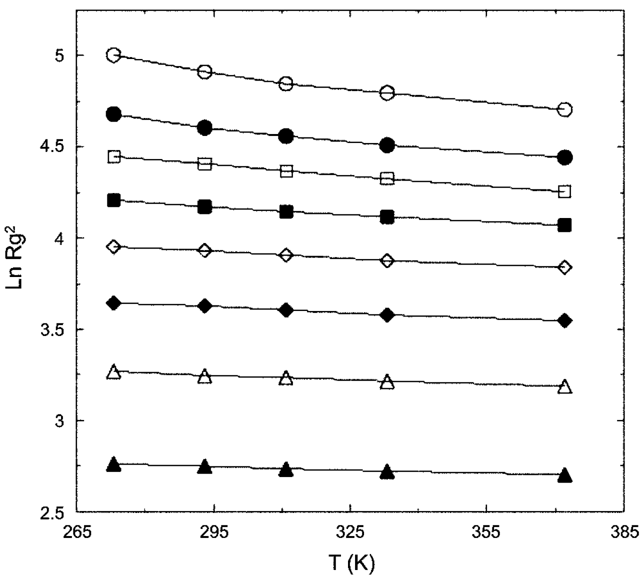

Figure 1. Plot of ($\ln R_g^2$) *vs*. temperature. From top, C_{44}, C_{36}, C_{32}, C_{28}, C_{24}, C_{20}, C_{16}, and C_{12}, respectively.

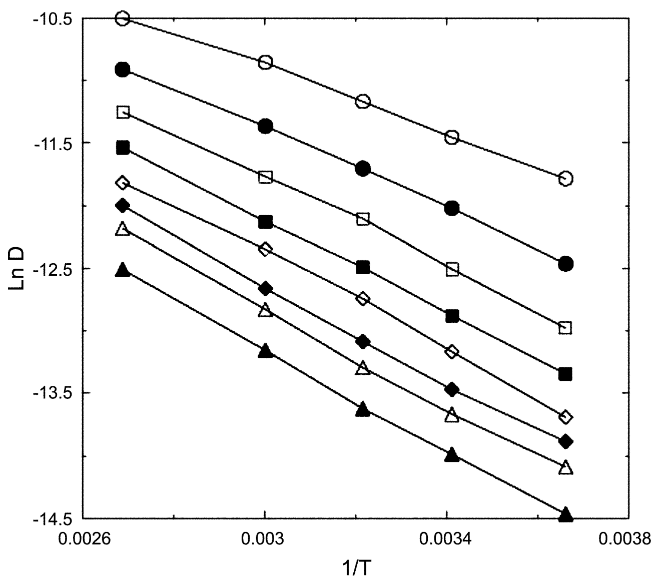

Figure 2. Arrhenius plot of self-diffusion constants versus inverse temperature for liquid *n*-alkanes. From top, C_{12}, C_{16}, C_{20}, C_{24}, C_{28}, C_{32}, C_{36}, and C_{44}, respectively.

mean square displacement (MSD) and the Green-Kubo relation Eq. (6), from the velocity autocorrelation (VAC) function of *n*-alkanes are collected in Table 2. The calculated diffusion constants of *n*-tetracosane (C_{24}) at 333 and 372 K are comparable with the pervious MD simulation results[22] for a united atom (UA) model [4.50(0.17) and 8.50(0.38) at 333 and 372 K, respectively], though these results overestimates the experimental measures [2.58 and 5.65 at 333 and 372 K, respectively].[28] The previous MD simulation study[22] could improve the results much better [2.70(0.11) and 5.50(0.21) at 333 and 372 K, respectively] by using an asymmetric united atom (AUA) model[29] which introduces a displacement between the centers of force of nonbonded interaction and the centers of mass of the united atoms. In this study we do not consider the use of the AUA model since the qualitative trend of diffusion constants of liquid *n*-alkanes may not vary much on the model property.

The temperature dependence of the calculated diffusion constants of liquid *n*-alkanes over the whole temperatures considered are suitably described by an Arrhenius plot:

$$D_{self} = D_0 \exp(-E_D/RT), \tag{5}$$

as shown in Figure 2, where D_0 is the pre-exponential factor, RT has the usual meaning, and E_D is the activation energy of *n*-alkane diffusion. The value of the activation energy is a direct measure of how fast the self-diffusion changes with temperature. The activation energies obtained from the slope of the least square fit are 2.66, 3.17, 3.53, 3.69, 3.84, 3.88, 3.93, and 4.01 kcal/mol for C_{12}, C_{16}, C_{20}, C_{24}, C_{28}, C_{32}, C_{36}, and C_{44}, respectively. The previous MD simulation study[22] reported this value as 3.98 kcal/mol for the UA model of *n*-tetracosane (C_{24}) which is compared with a value of 4.04 kcal/mol obtained from viscosity measurements[30] and a value of 4.36 from PFG NMR results.[31] We also show the log-log plot of diffusion constant versus molecular mass in Figure 3. The obtained exponents are between -1.6 and -2.1.

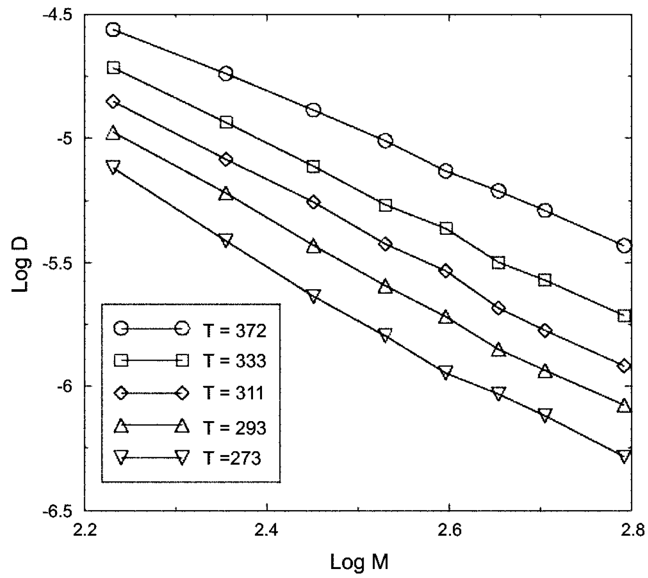

Figure 3. A log-log plot of self-diffusion constants versus molecular mass for liquid *n*-alkanes. From top, T = 372, 333, 311, 293, and 273 K, respectively.

Recent experimental study reported that $D_{self} \sim M^{-\alpha}$, with α changing approximately linearly from -2.72 to -1.85 as T increases.[7] Thus the apparent activation energies also rises linearly with log M. In the absence of molecular entanglements, Rouse kinetics predicts α = -1, but Cohen-Tumbull-Bueche free-volume effects due to molecular chain ends add a further nonpower-law term,[32] enhancing D increasingly at low M.

Global rotational motion. The global rotational motion of *n*-alkane molecules is characterized by the orientation relaxation of the end-to-end vector. Results are collected in Table 3, where τ_1 and τ_2 indicate the characteristic relaxation times of the first- and second-order orientation correlation

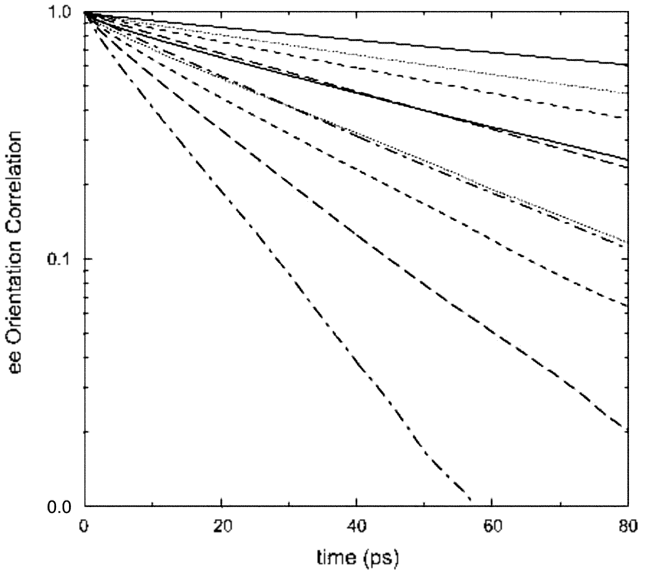

Figure 4. First-order (Eq. (6), upper curves) and second-order orientation correlation functions (Eq. (7), lower curves) of the end-to-end vector for *n*-dodecane (C_{12}). The solid, dotted, dashed, long dashed, and dot-dashed lines are for T = 273, 293, 311, 333, and 372 K, respectively.

functions,

$$P_1^{e1}(t) = \langle \mathbf{e}_1(t)\cdot\mathbf{e}_1(0)\rangle \tag{6}$$

and

$$P_2^{e1}(t) = \frac{1}{2}(3 < |\mathbf{e}_1(t)\cdot\mathbf{e}_1(0)|^2 > -1. \tag{7}$$

In Figure 4 we show the first- and second-order orientaion correlation functions (Eqs. (6) and (7)) of the end-to-end vector for *n*-dodecane (C_{12}) and *n*-tetracosane (C_{24}) at several temperatures. The relaxation behavior of the end-to-end vectors can always be adequately described by a simple exponential. The calculated characteristic relaxation times of *n*-tetracosane (C_{24}) at 333 and 372 K are comparable with the pervious MD simulation results[22] for a united atom (UA) model [531 and 211 for τ_1 and 215 and 92 for τ_2 at 333 and 372 K, respectively]. The characteristic relaxation time decreases with increasing temperature and it increases with increasing chain length. In the case of isotropic rotational diffusion a value of 3 for the ratio τ_1/τ_2 is expected.[33,34] The ratios τ_1/τ_2 obtained from the characteristic times given in Table 3 are the range between 2.63-2.82 for *n*-dodecane (C_{12}), 2.64-2.84 for *n*-tetracosane (C_{24}), and 2.60-2.63 for *n*-tetratetracontane (C_{44}) which are closed to 3. This ratio appears to decrease with increasing chain length which is contrasted with the decrease of the largest eigenvalues (I_1^2) of the mass tensor with chain length. It is hard to reach a detailed conclusion on the temperature and chain length dependence with given statistical uncertainty.

The Rouse model also predicts a relation for the relaxation of the time autocorrelation function of the end-to-end vector $\mathbf{R}_{ee}$ as[35]

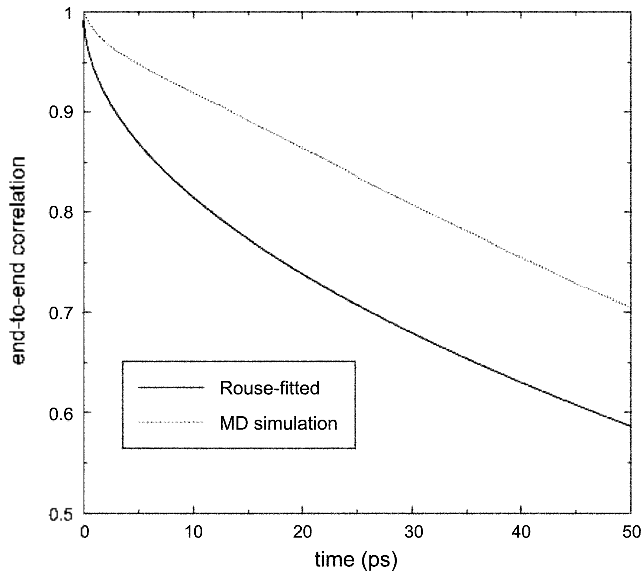

Figure 5. Time auto-correlation function of the end-to-end vector as extracted directly from the simulation and as calculated from Eq. (8) using τ_{ee} = 170 ps for *n*-dodecane (C_{12}) at 273 K.

$$\frac{\langle \mathbf{R}_{ee}(t)\cdot\mathbf{R}_{ee}(0)\rangle}{\langle R_{ee}^2\rangle} = \sum_{p=1,3,\ldots}\frac{8}{p^2\pi^2}\exp\left(-\frac{tp^2}{\tau_{ee}}\right) \tag{8}$$

where τ_{ee} is the longest relaxation time expressed as

$$\tau_{ee} = \frac{\zeta_0 n^2\langle R_{ee}\rangle^2}{3\pi^2 kT}, \tag{9}$$

where ζ_0 is the monomeric friction constant. This friction constant is related to the self-diffusion constant:

$$\zeta_0 = kT/nD_{self}. \tag{10}$$

From Eq. (8), it is obvious that the autocorrelation function of the end-to-end vector is clearly dominated by the first (p = 1) mode. In Figure 5 we compared the time auto-correlation function of the end-to-end vector as extracted directly from the simulation and as calculated from Eq. (8) using τ_{ee} = 170 ps for *n*-dodecane (C_{12}) at 273 K. The figure shows again that the short chain *n*-alkane is far away from the Rouse regime. Table 3 contains results of τ_{ee} calculated from the time auto-correlation function of the end-to-end vectors for *n*-dodecane (C_{12}), *n*-tetracosane (C_{24}), and *n*-tetratetracontane (C_{44}). The characteristic relaxation time decreases with increasing temperature and it increases with increasing chain length.

Friction constant. A friction constant is obtained from the time integral of the force auto-correlation function (FAC)[36,37]:

$$\zeta = \frac{1}{\tau_r} = \frac{1}{kT}\int_0^{\tau} dt\langle \mathbf{f}_i(t)\cdot\mathbf{f}_i(0)\rangle, \tag{11}$$

where $\mathbf{f}_i(t) = \mathbf{F}_i(t) - \langle\mathbf{F}_i(t)\rangle$, $\mathbf{F}_i(t)$ is the total force exerted on molecule i, and τ_r is the macroscopic relaxation time of the FAC.[37] The force auto-correlation functions obtained from

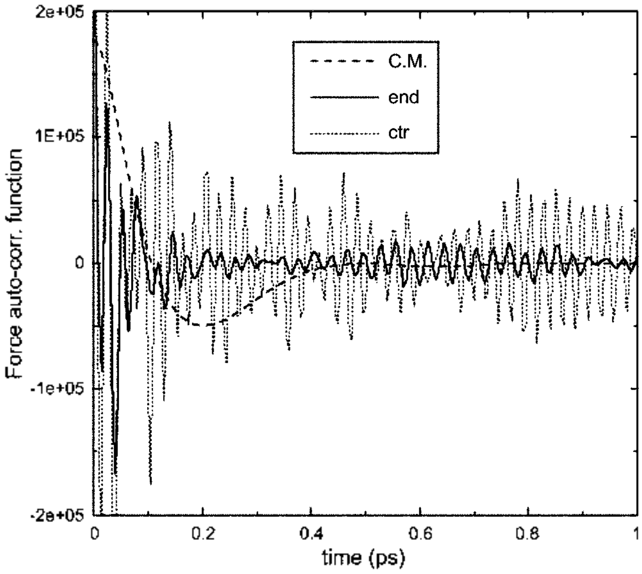

Figure 6. Force auto-correlation function of center of mass (dashed line), center monomer (dotted line), and end monomer (solid line) for *n*-dodecane (C_{12}) at 273 K.

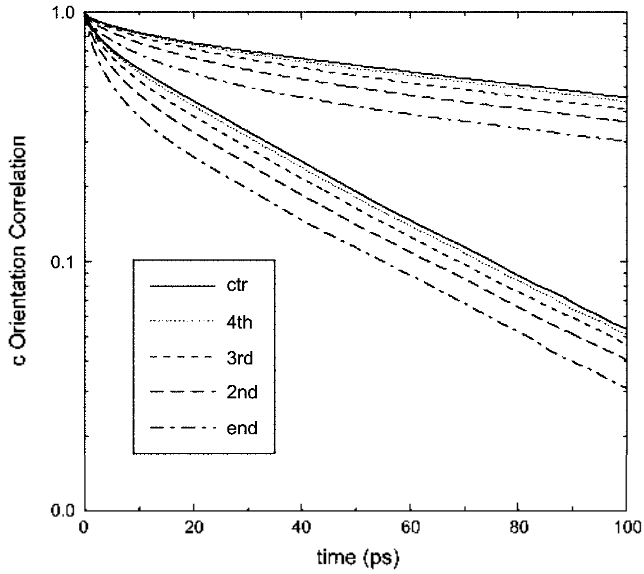

Figure 7. First-order orientation correlation functions (Eq. (6)) of the **c** vectors at different positions along the backbone for *n*-dodecane (C_{12}) at 273 K (upper curves) and at 372 K (lower curves).

our MD simulations for liquid *n*-tetracosane at 273.15 K only are shown in Figure 6. The FAC function for center of mass shows a well-behaved smoothly decaying curve, while those for center and end monomers are oscillating ones probably due to the rapidly varying interaction of methyl groups. The initial decay is very rapid, occurring in a time ~0.2 ps, while a subsequent long tail decays only after several ps(not shown). It is notorious that the calculation of friction constant from the force auto-correlation function is very hard due to the non-decaying long-time tails. As Kubo pointed out in his "fluctuation-dissipation theorem",[36] the correlation function of random force R will decay in a time interval of τ_c(microscopic time or collision duration time), whereas that of the total force F has two parts, the short time part or the fast similar to that of the random force and the slow part which should just cancel the fast part in the time integration.[38] This means that the time integral of Eq. (11) up to $\tau = \infty$ is equal to zero. The time integral in Eq. (11) attains a plateau value for τ satisfying $\tau_c << \tau << \tau_r$ if the upper limit of the time integral, Eq. (11), is chosen that $\tau_c << \tau << \tau_r$ because the slow tail of the correlation function is cut off. However, we were unable to get the plateau value in the running time integral of the force auto-correlation function. Kubo suggested above that the friction constants should be obtained from the random FAC function not from the total FAC and that there exists a difficulty to separate the random force part from the total force. We could obtain the friction constants by the time integral of the total FAC with choosing the upper limit of τ as the time which the FAC has the first negative value by assuming that the fast random force correlation ends at that time. The monomeric friction constant ζ_D is related to the diffusion constant D_{self} using Einstein relation (Eq. (3)) through Eq. (10). Table 2 contains the friction constants obtained from the time integral of the FAC using Eq. (11) and from Eq. (10) with D_{self} obtained from MSD's in Table 2. Both the friction constants give a correct qualitative trends: decrease with increasing temperature and increase with increasing chain length. The friction constant calculated from the FAC's using Eq. (10) decreases very slowly with increasing temperature, while the monomeric friction constant obtained from Eq. (10) varies rapidly with temperature.

Intramolecular dynamics and diffusion of the center and end monomers. We consider the orientation relaxation of three vectors in order to analyze the local intramolecular relaxation: the local orientation of the backbone (**c**), the perpendicular direction to the **c** vector in the local plane of the molecule (**a**), and the direction perpendicular to the molecular plane (**b**). The orientation relaxation of these local vectors are considered at both the center and end of the molecule. In a chain of *n* sites numbered from 1 to *n*, for example, the end **c** vectors represent $\mathbf{c} = \mathbf{r}_1\text{-}\mathbf{r}_3$ and $\mathbf{c} = \mathbf{r}_{n-2}\text{-}\mathbf{r}_n$, and the center c vectors $\mathbf{c} = \mathbf{r}_{n/2-1}\text{-}\mathbf{r}_{n/2+1}$ and $\mathbf{c} = \mathbf{r}_{n/2}\text{-}\mathbf{r}_{n/2+2}$. In Figure 7 we show the first-order orientation correlation functions (Eq. (6)) of the **c** vectors at different positions along the backbone for *n*-dodecane (C_{12}) at 273 K and at 372 K. Note that the relaxation behavior of the **c** vectors is adequately described by a simple exponential. Table 3 contains results of τ_1 calculated from the time auto-correlation function of these local vectors at both the center and end of *n*-dodecane (C_{12}), *n*-tetracosane (C_{24}), and *n*-tetratetracontane (C_{44}). The orientation relaxation time decreases with increasing temperature. In general the orientation of the **b** and **a** vector relaxes much shorter than that of the corresponding **c** vector, while there is a little difference between **b** and **a**. In the case of *n*-dodecane (C_{12}), the orientation relaxation times of the three vectors for the center and end monomers are almost the same, reflecting the rigidity of the backbone, while for *n*-tetracosane (C_{24}) and *n*-tetratetra-

Table 4. Self-diffusion constants calculated from MSD's and monomeric friction constants of each site of n-$C_{12}H_{26}$ and n-$C_{24}H_{50}$ at 273 K. Uncertainties in the last reported digit(s) are given in parenthesis

n-alkanes	Site	D_{self} (MSD)^a	$\zeta_{D(MSD)}$^{b}	Site	D_{self} (MSD)	$\zeta_{D(MSD)}$
n-$C_{12}H_{26}$	end	12.4(4)	153(10)	2nd	11.0(4)	172(13)
	3rd	9.80(46)	193(18)	4th	8.91(45)	212(22)
	5th	8.34(46)	227(25)	ctr	8.06(46)	235(27)
n-$C_{24}H_{50}$	end	4.69(17)	202(15)	2nd	3.93(14)	241(17)
	3rd	3.37(15)	281(26)	4th	3.07(13)	308(26)
	5th	2.88(12)	329(27)	6th	2.82(17)	336(41)
	7th	2.77(15)	342(37)	8th	2.76(21)	343(52)
	9th	2.78(21)	340(52)	10th	2.79(25)	339(61)
	11th	2.77(25)	342(62)	ctr	2.78(25)	340(62)

^{a}In 10^{-6} cm^2/sec. ^{b}In g/(ps·mol).

contane (C_{44}) the relaxations in the end vectors are much faster than in the center, indicating a significant degree of flexibility of the molecular ends. The relative difference in the orientation relaxation time between the center and end vectors is slightly larger in the **b** and **a** vectors than in the corresponding **c** vector.

We have also examined diffusion behavior of each site of n-dodecane (C_{12}) and n-tetracosane (C_{24}) at 273 K. Table 4 contains self-diffusion constants of each site calculated from mean square displacement (MSD) through the Einstein relation, Eq. (3), and monomeric friction constants calculated from Eq. (11). We were not able to calculate the friction constants of each site directly from the force auto-correlation (FAC) functions, since these functions are oscillating fast probably due to the rapidly varying interaction of methyl groups as shown Figure 6. Self-diffusion constants of all sites are generally larger than that of center of mass which is listed in Table 2, and diffusive motion of the end monomers are much larger than the center monomer. As the site is closer to the center, diffusive motion becomes smaller. In the case of n-tetracosane (C_{24}), several sites close to the center show almost the same self-diffusion constant indicating that the center part of a long chain retains a considerable degree of rigidity. Roughly speaking, rotational and translational diffusion of the ends are faster than those of the center.

Conclusion

In this paper we have presented the results of diffusion behavior of model systems for eight liquid n-alkanes in a canonical (NVT) ensemble at 273, 293, 311, 333, and 372 K using molecular dynamics simulations. Diffusion dynamics of these n-alkanes of small chain length n is well understood using the united atom model with relatively small deviation from the experimental diffusion constants. The small chains of these n-alkanes are clearly $\langle R_{ee}^2\rangle/6\langle R_g^2\rangle > 1$ and non-Gaussian. This result implies that the liquid n-alkanes over the whole temperatures considered are far away from the Rouse regime, though the ratio becomes close to the unity as n increases. Calculated self-diffusion constants D_{self} are comparable with experimental results and the Arrhenius plot of self-diffusion constants versus inverse temperature shows a different temperature dependence of diffusion on the chain length. The comparison of the time auto-correlation function of the end-to-end vector as extracted directly from the simulation and as calculated from using τ_{ee}=170 ps for n-dodecane (C_{12}) at 273 K also supports this conclusion. The local intramolecular relaxation is also analyzed by considering the orientation relaxation of three local vectors, and diffusion and friction of each site are examined to show that rotational and translational diffusions of the ends are faster than those of the center.

Acknowledgment. This research was supported by a Korea Research Foundation Grant (KRF-2000-015- DP0185). This research is a partial fulfillment of the requirements for the degree of Ph. D. of Science for GHG at Department of Chemistry, Graduate School, Kyungsung University.

References

1. Ferry, J. D. *Viscoelastic Properties of Polymers*, 3rd ed.; Wiley: New York, 1980.
2. Berry, G. C.; Fox, T. G. *Adv. Polym. Sci.* **1968**, *5*, 261.
3. Lodge, T. P.; Rotstein, N. A.; Prager, S. *Adv. Chem. Phys.* **1990**, *9*, 1.
4. De Gennes, P.-G. *Scaling Concepts in Polymer Physics*; Cornell University Press: Ithaca, New York, 1979.
5. Fleisher, G. *Polym. Bull. (Berlin)* **1983**, *9*, 152.
6. Pearson, D. S.; Ver Strate, G.; von Meerwall, E.; Schilling, F. C. *Macromolecules* **1987**, *20*, 1133.
7. Von Meerwall, E.; Beckman, S.; Jang, J.; Mattice, W. L. *J. Chem. Phys.* **1998**, *108*, 4299.
8. Harmandaris, V. A.; Mavrantzas, V. G.; Theodorou, D. N. *Macromolecules* **1998**, *31*, 7934.
9. Mondello, M.; Grest, G. S.; Webb, E. B.; Peczak, P. *J. Chem. Phys.* **1998**, *109*, 798.
10. Park, H. S.; Chang, T.; Lee, S. H. *J. Chem. Phys.* **2000**, *113*, 5502.
11. Evans, D. J.; Hoover, W. G.; Failor, B. H.; Moran, B.; Ladd, A. J. C. *Phys. Rev. A* **1983**, *28*, 1016.
12. Simmons, A. D.; Cummings, P. T. *Chem. Phys. Lett.* **1986**, *129*, 92.
13. Siepmann, J. I.; Karaborni, S.; Smit, B. *Nature (London)* **1993**, *365*, 330.
14. Smit, B.; Karaborni, S.; Siepmann, J. I. *J. Chem. Phys.* **1995**, *102*, 2126.
15. Mundy, C. J.; Siepmann, J. I.; Klein, M. L. *J. Chem. Phys.* **1995**, *102*, 3376.
16. Cui, S. T.; Cummings, P. T.; Cochran, H. D. *J. Chem. Phys.* **1996**, *104*, 255.
17. Cui, S. T.; Gupta, S. A.; Cummings, P. T.; Cochran, H. D. *J. Chem. Phys.* **1996**, *105*, 1214.
18. Jorgensen, W. L.; Madura, J. D.; Swenson, C. J. *J. Am. Chem. Soc.* **1984**, *106*, 6638.
19. Gear, C. W. *Numerical Initial Value Problems in Ordinary Differential Equation*; Englewood Cliffs, NJ: Prentice-Hall, 1971.
20. Andersen, H. *J. Comput. Phys.* **1984**, *52*, 24.
21. McQuarrie, D. A. *Statistical Mechanics*; Harper and Row: New York, 1976.
22. Mondello, M.; Grest, G. S. *J. Chem. Phys.* **1995**, *103*, 7156.
23. Baschnagel, J.; Qin, K.; Paul, W.; Binder, K. *Macromolecules* **1992**, *25*, 3117.
24. Brown, D.; Clarke, J. H. R.; Okuda, M.; Yamazaki, T. *J. Chem.*

Phys. **1994**, *100*, 1684; *ibid* **1996**, *104*, 2078.
25. Paul, W.; Smith, G. D.; Yoon, D. Y. *Macromolecules* **1997**, *30*, 7772.
26. Boothroyd, A.; Rennie, A. R.; Boothroyd, C. B. *Europhys. Lett.* **1991**, *15*, 715.
27. Goldstein, *Classical Mechanics*; Addison-Wesley: Harvard University, 1974;, p 155.
28. See Table IV in Reference 22.
29. Padilla, P.; Toxvaerd, S. *J. Chem. Phys.* **1991**, *94*, 5650; *Ibid* **1991**, *95*, 509.
30. Nederbragt, G. W.; Boelhouwer, J. W. M. *Physica* **1947**, *13*, 305.
31. See page 7161 in Reference 22.
32. Doi, M.; Edwards, S. F. *The Theory of Polymer Dynamics*; Clarendon: Oxford, 1986.
33. Debye, P. *Polar Molecules*; Dover: New York, 1929.
34. Berne, B.; Pecora, R. *Dynamic Light Scattering*; Wiley: New York, 1976.
35. Cohen, M. H.; Turnbull, D. *J. Chem. Phys.* **1959**, *31*, 1164.
36. Ciccotti, G.; Ferrario, M.; Hynes, J. T.; Kapral, R. *J. Chem. Phys.* **1990**, *93*, 7137.
37. Kubo, R. *Rep. Prog. Phys.* **1966**, *29*, 255.
38. Kubo approximately described these two force auto-correlation functions in his original papers, see Fig. 2 in Ref. 37.